PNAS INAUGURAL ARTICLE | ENVIRONMENTAL SCIENCES

The metabolic rate of the biosphere and its components

Tori M. Hoehler[a], Dylan J. Mankel[a,b], Peter R. Girguis[c], Thomas M. McCollom[d], Nancy Y. Kiang[e], and Bo Barker Jørgensen[f,1]

This contribution is part of the special series of Inaugural Articles by members of the National Academy of Sciences elected in 2020.

Contributed by Bo Barker Jørgensen; received March 6, 2023; accepted April 26, 2023; reviewed by Ron Milo and Kenneth H. Nealson

We assessed the relationship between rates of biological energy utilization and the biomass sustained by that energy utilization, at both the organism and biosphere level. We compiled a dataset comprising >10,000 basal, field, and maximum metabolic rate measurements made on >2,900 individual species, and, in parallel, we quantified rates of energy utilization, on a biomass-normalized basis, by the global biosphere and by its major marine and terrestrial components. The organism-level data, which are dominated by animal species, have a geometric mean among basal metabolic rates of 0.012 W $(g\ C)^{-1}$ and an overall range of more than six orders of magnitude. The biosphere as a whole uses energy at an average rate of 0.005 W $(g\ C)^{-1}$ but exhibits a five order of magnitude range among its components, from 0.00002 W $(g\ C)^{-1}$ for global marine subsurface sediments to 2.3 W $(g\ C)^{-1}$ for global marine primary producers. While the average is set primarily by plants and microorganisms, and by the impact of humanity upon those populations, the extremes reflect systems populated almost exclusively by microbes. Mass-normalized energy utilization rates correlate strongly with rates of biomass carbon turnover. Based on our estimates of energy utilization rates in the biosphere, this correlation predicts global mean biomass carbon turnover rates of ~2.3 y^{-1} for terrestrial soil biota, ~8.5 y^{-1} for marine water column biota, and ~1.0 y^{-1} and ~0.01 y^{-1} for marine sediment biota in the 0 to 0.1 m and >0.1 m depth intervals, respectively.

metabolic rate | mass-specific power | energy metabolism | global energy budget

Significance

Assessing the relationship between energy flux and the quantity of biomass it sustains offers the potential to understand the biological "carrying capacity" for ecosystems on Earth and beyond. Our work supports this understanding by quantifying the energy–biomass relationship for the global biosphere and an environmentally diverse range of its components, and by exploring the factors—including the impact of humanity—that affect that relationship.

Energy is required by all life to fuel growth and activity, including the maintenance of viability in existing biomass. Accordingly, the availability of energy constrains the potential abundance, distribution, and productivity of life.

An extensive body of work has been devoted to quantifying rates of energy utilization by individual species and to exploring the dependence of those rates on body mass as well as extrinsic factors such as temperature. These studies reflect the range of metabolic potential—what rates of energy utilization are required, and what rates are possible—when considering a broad range of organisms. In nature, however, the relationship between biomass and energy utilization rate depends on how organisms' metabolic potential is expressed in the context of ecological interactions, life cycles, and variable if not challenging extrinsic factors that are not necessarily encompassed in measurements made on individuals.

In this study, we aim to quantify and understand the relationship between biomass and energy utilization rate—hereafter termed "mass-specific power" (MSP), with units of energy consumed per unit time per unit biomass [W $(g\ C)^{-1}$]—for the biosphere overall and for its major marine and terrestrial components. We estimated rates of biological energy utilization in each of these components and combined them with existing estimates of biomass to compute MSP. In parallel, we compiled a database of >10,000 metabolic rate measurements made on >2,900 species. The results provide two fully independent but complementary assessments of MSP, with the database reflecting the scope of physiological potential in organisms, and the biosphere level calculations reflecting the expression of that potential in different environments.

Results

A number of previous studies compiled datasets ranging from hundreds to thousands of metabolic rate measurements (e.g., refs. 1–7). We combined and augmented these datasets, eliminating any resulting duplicate entries, to assemble a set of ~10,500 individual metabolic rate measurements, representing 2,912 species (Dataset S1). The complete source literature for Dataset S1 is given in *SI Appendix*, Table S1. To support comparison across the diversity of metabolic rate measurements in the dataset, all rates were converted to the common power unit of Watts (Joule s^{-1}). This also provides a common basis for comparing metabolic rate measurements made on individuals to estimates of energy

Author affiliations: [a]Exobiology Branch, NASA Ames Research Center, Moffett Field, CA 94035; [b]Department of Biology, Boston University, Boston, MA 02215; [c]Department of Organismic and Evolutionary Biology, Harvard University, Cambridge, MA 02138; [d]Laboratory for Atmospheric and Space Physics, University of Colorado, Boulder, CO 80309; [e]NASA Goddard Institute for Space Studies, New York, NY 10025; and [f]Department of Biology, Aarhus University, Aarhus C 8000, Denmark

Author contributions: T.M.H. and B.B.J. designed research; T.M.H., D.J.M., P.R.G., T.M.M., N.Y.K., and B.B.J performed research; D.J.M. contributed new reagents/analytic tools; T.M.H., D.J.M., T.M.M., N.Y.K., and B.B.J. analyzed data; and T.M.H., P.R.G., T.M.M., and B.B.J. wrote the paper.

Reviewers: R.M., Weizmann Institute of Science; and K.H.N., University of Southern California.

The authors declare no competing interest.

[1]To whom correspondence may be addressed. Email: bo.barker@bio.au.dk.

This article contains supporting information online at https://www.pnas.org/lookup/suppl/doi:10.1073/pnas.2303764120/-/DCSupplemental.

Published June 12, 2023.

utilization rate by the biosphere and its components. While Dataset S1 includes species from across the entire tree of life, it is dominated by animals, for which the majority of measurements have been made. We hereafter refer to these data, for which metabolic rate and MSP can be attributed to an individual species, as "organism-level" rates or MSP.

The literature on animal metabolic rates distinguishes three measurement types, all of which are represented in the dataset. Basal rates, sometimes called standard rates, are measured in nongrowing, fasting and resting organisms held within their natural temperature range (8). We also include "endogenous" rates (for microorganisms) and dark respiration rates (for phototrophic organisms) within the basal rate category, following the approach of ref. 2. Endogenous rates are those measured when microorganisms are held in culture without exogenous substrates (9). Basal rates dominate the literature and, therefore, our dataset. Field rates are measured on organisms in their normal environment and encompass a full range of normal activity (10). Maximum rates are measured at peak physical activity or, for microorganisms, during exponential growth under optimal conditions.

The complete set of metabolic rate data (Dataset S1) can be visualized in an interactive plot (see Supplementary Interactive Plot or https://doi.org/10.5281/zenodo.7877885) in which the user can toggle between: a) metabolic rate or mass-specific metabolic rate; b) wet biomass, dry biomass, or carbon biomass units; c) basal, field, and/or maximum metabolic rates; and d) metabolic rates that are or are not normalized from measurement temperature to 25 °C via a Q_{10} calculation. Further information on the interactive plot is given in *SI Appendix*.

Power and MSP at the Organism Level. Fig. 1 presents "snapshots" from the Supplementary Interactive Plot of metabolic power vs. mass (Fig. 1*A*) and mass-specific metabolic power (MSP) vs. mass (Fig. 1*B*) for a specific configuration that includes basal rates only, with no temperature normalization, and using carbon-based mass units. Fig. 1*A* shows that the basal metabolic power of individuals scales with carbon biomass (g) across ~22 orders of magnitude ($<10^{-14}$ to $>10^{7}$ g C) according to a power law:

$$\text{Metabolic power (W)} = 0.0104 \times (\text{g C})^{0.95} \quad [1]$$

The exponent, $k = 0.95 \pm 0.003$, is close to unity and shows that the metabolic rates vary nearly proportionally to the biomass of the organisms, when viewed over the entire tree of life. This stands in contrast to the well-documented scaling of basal metabolic rates with mass in some taxa such as mammals ($k = 0.73$), birds ($k = 0.67$ to 0.74), fishes ($k = 0.86$), and insects ($k = 0.66$) (e.g., refs. 11–13). Within these taxa, metabolic power increases relatively less than the increase in biomass. These trends become clearer when metabolic power is normalized to body mass (Fig. 1*B*). Among the mammals or birds, mass-specific metabolic power (MSP) exhibits a systematic 100-fold decrease with increasing body mass, from pygmy shrew to blue whale or from hummingbird to ostrich.

When considering maximum MSP (Fig. 1*B* ovals) in addition to basal MSP, with no temperature normalization, the data span more than six orders of magnitude, to nearly 4,500-fold above and 850-fold below the basal geometric mean of 0.012 W $(\text{g C})^{-1}$ (Fig. 1*B* and Supplementary Interactive Plot). Yet, about two-thirds

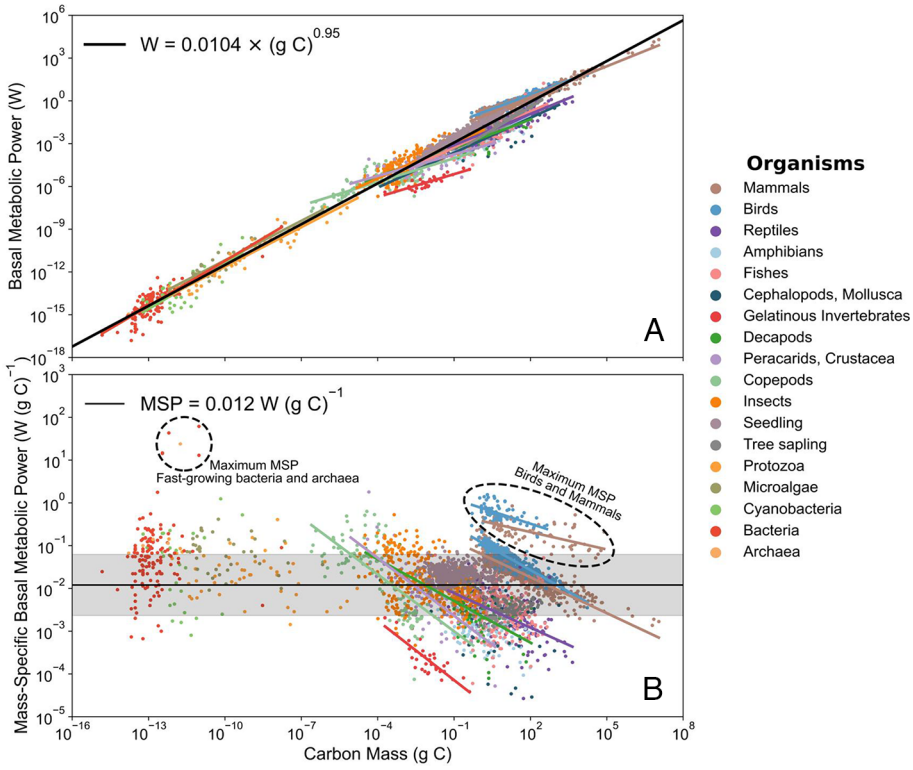

Fig. 1. (*A*) Basal metabolic power vs. biomass carbon calculated from metabolic rate measurements made on 2912 species. The solid black line is a power law fit to the entire dataset. (*B*) Mass-specific basal metabolic power (MSP) vs. biomass carbon. The solid black line and shaded region are, respectively, the geometric mean and SD (fivefold) among all species. In both panels, the solid, colored lines are log-log-linear correlations for specific taxonomic groups, identified by the color codes of "Organisms." The ranges of maximum MSP for birds and mammals and for prokaryotes are denoted by dashed ovals. Note that the maximum MSP range denoted for prokaryotes is specific to a small group of fast-growing organisms and does not represent a broad survey of maximum prokaryote rates. An interactive version of this plot is accessible as "Supplementary Interactive Plot" or at https://doi.org/10.5281/zenodo.7877885.

of all data cluster within fivefold of the mean. Normalizing all data to 25 °C narrows the full range of MSP by only fivefold. This is notable because, given measurement temperatures ranging from ~0 to 72 °C, temperature normalization could potentially contract that range by more than 100-fold. The uppermost 1.5 orders of magnitude in the MSP range are occupied exclusively by prokaryotes growing in cultures with substrates and nutrients present in abundance, with population doubling times in the range of hours or less ("maximum MSP," Fig. 1*B*). Conversely, the lowermost order of magnitude in MSP is occupied predominantly by aquatic animals, including the painted turtle and vampire squid. Microorganisms in energy-poor natural settings likely subsist with even lower MSP (see *Discussion*: The Range of MSP), but we limit our dataset, and the data represented in Fig. 1, to metabolic rate measurements that can be attributed to individual taxa rather than mixed natural populations.

Power and MSP at the Biosphere Level. We estimated annually averaged rates of energy utilization (power) by the global biosphere and its components (Table 1) based on published estimates of global marine and terrestrial gross and net primary productivity (GPP and NPP), autotrophic respiration, and soil and seabed respiration. Data sources and the methods for conversion to units of power are described briefly in "*Materials and Methods*" and in detail in *SI Appendix*, section 3. For primary producers, two distinct quantities are reported: i) "photon capture" refers to the total energy of photons that are absorbed and subsequently regenerate ATP and reducing power through entrainment into the light reactions of photosynthesis; it excludes photon energy that is absorbed but lost to heat or fluorescence without driving electron transfers. This term is a measure of the captured light energy that ultimately drives the productivity of our planet. ii) "Autotrophic resp." refers to the power generated by phototrophic organisms through respiration of a fraction of the carbon that is fixed during photosynthesis. This term most closely approximates the MSP reported for phototrophic species in the organism-level data and provides a more direct basis for comparison with animals and microorganisms that fuel their metabolisms by respiration. For marine and terrestrial heterotrophic "consumers" (animals and nonphotosynthetic microorganisms), we report the power generated by aerobic or anaerobic respiration of organic carbon derived from photosynthetic NPP.

The global photosynthetic biosphere harnesses about 2,800 TW of light energy via photosynthesis (i.e., as "photon capture"),

Table 1. Estimates of mass (Pg = 10^{15} g), power (TW = 10^{12} Watt), and MSP for the global biosphere

	Mass (Pg C)*	Uncertainty	Power (TW)	Uncertainty (SD)	MSP (W/g C)	Uncertainty
Global total	510	1.2-fold	2,800	270	0.0054	1.2-fold
Marine						
Producers (photon capture)	0.53†	3.2-fold	1,200	130	2.3	3.2-fold
Producers (autotrophic resp.)	0.53†	3.2-fold	90	20	0.18	3.3-fold
Consumers, pelagic	5	3.3-fold	57	5	0.011	3.4-fold
Consumers, sediments 0 to 0.1m	2.3‡	2.1-fold	3	0.8	0.0013	2.3-fold
Consumers, sediments > 0.1m	4.1§	3.2-fold	0.07	—	0.00002	—
Terrestrial						
Producers (photon capture)						
Total mass	450¶	± 50	1,600	240	0.0036	± 0.0007
Active tissue#	200	—	1,600	240	0.01	—
Producers (autotrophic resp.)						
Total mass	450¶	± 50	80	20	0.0002	± 0.00005
Active tissue#	200	—	80	20	0.0005	—
Consumers, soils 0 to 8m	20	1.9-fold	50	13	0.0025	2.1-fold
Consumers, deep biosphere	27‖	± 4‖	—	—	—	—
Humanity (metabolic)	0.09‡	± 0.04	1.07**	0.005	0.012	± 0.005
Humanity (technological)	0.09‡	± 0.04	18.5††	0.005	0.21	± 0.09
Livestock	0.10	± 0.015	3.9	0.4	0.039	± 0.007
Geochemical						
Marine	—	—	0.03	—	—	—
Terrestrial	—	—	0.005	—	—	—

*Except where noted, mass and uncertainty estimates are from ref. 14.
†From ref. 15, based on a wet mass of 5.3 Pg and wet-to-carbon mass conversion factor of 10:1. This estimate is specific to pelagic primary producers (i.e., phytoplankton) and does not include benthic primary producers such as coastal sea grasses.
‡This study.
§Ref. 16.
¶Ref. 17.
#Noting that woody tissue may comprise a significant fraction of plant biomass, the designation "Active tissue" denotes an estimate of the portion of total plant biomass that represents metabolically active tissue, which (14) took to be one-third. As there is no estimate of uncertainty for this fraction, we express mass and MSP with only one significant digit and do not calculate an uncertainty estimate for the associated MSP.
‖Ref. 18 gives a range of 23 to 31 Pg C, which we take to be 27 ± 4 Pg C.
**Calculated from UN-FAO data for global population and average per-capita dietary intake.
††Ref. 19.

which is ~3% of the global full spectrum solar irradiance at Earth's surface and ~7% of the available photosynthetically active radiation (PAR). The combined gross primary productivity (GPP) of marine and terrestrial primary producers, about 220 to 340 Pg C y^{-1} (20, 21), represents a chemical energy flux of 280 TW when utilized in respiration, of which 170 TW is attributable to autotrophic respiration in phototrophs and 110 TW is attributable to heterotrophic respiration by Earth's nonphotosynthetic biota*.

For the oceans, we estimated separate rates of energy utilization by primary producers (phytoplankton) and secondary and tertiary producers (heterotrophic organisms) within the water column, the upper 0.1 m of seafloor sediments, and sediments beneath 0.1 m. Marine primary producers account for a little over 40% of global photosynthetic energy capture. This measure is specific to chlorophyll-based photosynthesis (22), and recent work suggests that rhodopsin-based phototrophy could contribute significantly to the capture of light energy in the oceans (23); hence, the entries for marine primary producer power and MSP in Table 1 are potentially underestimates. Across the succession from marine primary producers to pelagic, shallow sediment, and deep sediment consumers, energy flux diminishes systematically by 10^5-fold, even though the standing biomass varies by only an order of magnitude (Table 1). Of the total power generated by heterotrophic respiration of marine NPP, pelagic biota account for 95%, with most of the remaining 5% accessed by biota in the 0 to 0.1 m sediment interval. Respiration in sediments beneath the 0.1 m horizon accounts for only about 0.1% of the total power.

On the continents, estimates can be made of energy utilization by primary producers (plants and alga), heterotrophic soil biota, humanity, and livestock. We could not determine global rates of energy utilization by the terrestrial deep biosphere or by wild animals that are not soil associated (e.g., wild birds, mammals, and some arthropods), but it is likely that these groups account for only a small fraction of terrestrial heterotrophic respiration (*SI Appendix*, section 3.2). Soils consume about 80% of all terrestrial NPP (24) and, noting that some NPP is lost to nonbiological processes such as fires and wood trade (24), account for 90% of the total power generated by heterotrophic respiration of terrestrial NPP. This highlights an important distinction between soils, which receive a direct flux of terrestrial NPP through litter and roots, and marine sediments, which receive only the small fraction of marine NPP that escapes consumption in the water column. In this regard, soils (50 TW) are more comparable to the pelagic ocean (57 TW) than to marine sediments. Humanity and livestock combined represent < 0.5% of the total mass of terrestrial heterotrophic consumers (when including both soil biota and the terrestrial deep biosphere) but account for about 10% of the total metabolic power generated by heterotrophic respiration of terrestrial NPP. Humanity's technological utilization of energy exceeds its metabolic utilization by 17-fold.

To distinguish the relative importance of solar energy from geochemical sources of energy (the so-called dark energy that is independent of solar energy), we estimated the major geochemical fluxes of reductants that could be utilized by microorganisms (*SI Appendix*, Table S4). If all such fluxes were completely consumed via aerobic metabolism, the resulting power would be 0.03 TW in the oceans and 0.005 TW on the continents (Table 1 and *SI Appendix*, Table S5). Combined, these are nearly 5 orders of magnitude less than global photosynthetic energy capture and would be lower still in the absence of photosynthetically produced oxygen, because oxidation of these reductants with O_2 yields considerably more energy than with non-O_2 oxidants.

*Comparison between global GPP (280 Pg C y^{-1}) and the "photon capture" and "autotrophic resp" metrics of power (2,800 TW and 280 TW, respectively) suggests the rule-of-thumb approximations that 10 Joules of captured solar energy yields a quantity of photosynthetically fixed carbon equivalent to 1 Joule of chemical energy (when respired with oxygen), and that a respiration rate of 1 kg C y^{-1} represents a power of 1 W.

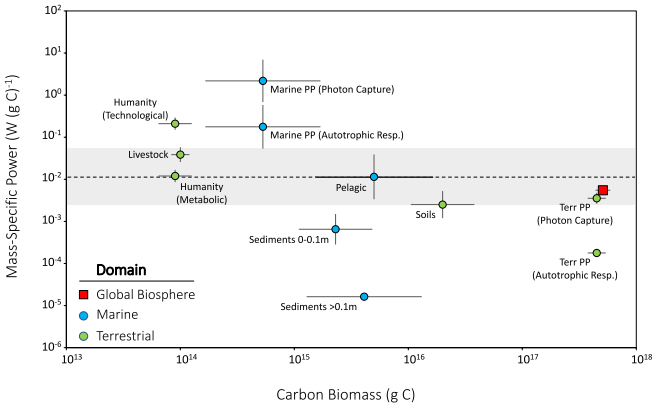

Fig. 2. Mass-specific power vs. carbon biomass for the global biosphere (red square) and for its marine and terrestrial components (blue and green circles, respectively). For marine and terrestrial primary producers (PP), the parenthetical designation "Photon Capture" refers to the total energy of photons captured into the light reactions of photosynthesis, while "Autotrophic Resp." refers to the power provided by autotrophic respiration of photosynthetically fixed carbon. The dashed line and shaded region are, respectively, the all-species geometric mean and SD taken from the organism-level data (Fig. 1*B*), while vertical and horizontal error bars reflect the uncertainties shown in Table 1.

MSP at the biosphere level. For the various components of the biosphere, MSP is calculated from our energy flux estimates as well as published estimates of biomass for those components (Table 1). These calculations are completely independent from the MSP determined at the organismal level (i.e., the data in Fig. 1), and we hereafter refer to the calculated values as "biosphere-level MSP." Operationally, the biosphere-level MSP estimates are more comparable to metabolic "field rates" measured at the species level but they differ by integrating across species, ecological niches, temperatures, and the full life cycle of growth, reproduction, and death.

We estimate the mean MSP for the global biosphere at 0.005 W (g C)$^{-1}$, or about 1 W (kg wet mass)$^{-1}$, which is within ~twofold of the all-species basal mean MSP [0.012 W (g C)$^{-1}$; Fig. 1*B*]. This calculation factors in the complete biomass of plants, including woody tissue. When considering only the metabolically active fraction of plant biomass, which Bar-On et al. (14) estimate to be roughly one-third of total mass, global MSP then approximates the all-species mean at ~0.01 W (g C)$^{-1}$. Such close agreement is surprising, in that the organism-level data are dominated by the basal metabolic rates of animals (Fig. 1), while global MSP is dominated in power terms by the "photon capture" energy harvesting of oceanic and terrestrial primary producers and in mass terms by trees and microorganisms (Table 1).

Among the components of the biosphere considered in this study, MSP spans the same five order of magnitude range that is encompassed in the organism-level basal MSP data (compare Fig. 2 and Fig. 1B). The entire range of biosphere-level MSP is encompassed in the four "compartments" of the microbe-dominated marine biosphere, where biomass varies within only an order of magnitude despite a systematic five order of magnitude decrease in power from the phototrophic top of the water column to the deep subseafloor biosphere (Fig. 2). The terrestrial biosphere behaves in largely orthogonal fashion: Decreasing power is accompanied by corresponding decreases in biomass, such that MSP varies only 13-fold across the 4,500-fold range in carbon biomass that encompasses primary producers, soil biota, humanity, and

livestock (Fig. 2). All lie within about sixfold of the all-species mean (Fig. 2, dashed line). It is likely that the terrestrial deep biosphere (data not available) operates with considerably lower MSP than shallow soil so that the terrestrial MSP could span 3+ orders of magnitude.

Discussion

Our objective in this work is to quantify MSP, and to understand the factors that control it, at the biosphere level—where it integrates across biological diversity, life stages, and a range of environmental (including ecological) factors. The rich body of literature dedicated to documenting the factors that control MSP at the organism level and within specific taxa provides a strong basis from which to understand its expression at the biosphere level. The challenge is to extrapolate beyond a heavy focus on animals that ultimately account for only a minor fraction of energy consumption and mass at the biosphere level, and beyond experimental conditions that do not capture all factors that impact physiological status in natural settings. A particular challenge is to map our organism-level understanding of MSP to the microbial communities that dominate the biomass of terrestrial soils as well as the four components of the marine biosphere that we considered.

The Range of MSP. Across the various components of the biosphere, MSP spans five orders of magnitude (Fig. 2). This range is a function of both the potential that exists at a physiological level and how that potential is expressed in the environment. An expansive literature describes the factors responsible for the realized MSP of individual animal species and, therefore, the ~five order of magnitude range in MSP that is observed across animals overall (Fig. 1*B*). However, at the biosphere level, the extremes in MSP are attributable to the dynamics of microbe-dominated systems.

Multicellularity influences the upper, and possibly the lower, absolute limits of animal and plant MSP. For example, among animals with the highest known MSPs (e.g., hummingbirds), cardiac output and mitochondrial enzyme packing very likely constrain the absolute upper limit of aerobic respiration (25, 26). To date, a few studies have also considered the energetic costs (and benefits) of multicellularity, such as the maintenance of tissue organization and differentiation and cellular diversification (27). By imposing a minimal energetic cost on the maintenance of a multicellular form, such factors may set the lower limits of animal MSP, though to our knowledge this remains to be substantiated.

Microorganisms, including bacteria, archaea, and unicellular eukaryotes, exhibit a considerably larger range in MSP than animals do. When considering maximum MSP (Fig. 1*B*), the microorganisms in our database extend ~1.5 orders of magnitude beyond the uppermost values for animals. Conversely, animals exhibit the lowest basal MSP in our dataset, but this likely reflects challenges in cultivating microorganisms at very low metabolic rates rather than a true lack of microorganisms capable of subsisting at low MSP. Several studies have independently estimated cell-specific power on the order of 10^{-19} to 10^{-20} W cell^{-1} for deep sediment microorganisms (28–31). For a mean cell mass of 14 fg C for deep sediment microbes (16), this equates to an MSP of 7×10^{-7} to 7×10^{-6} W (g C)$^{-1}$ – about 1.5 orders of magnitude below the lowest values measured for animals. If these values are included, MSP for microorganisms spans an overall range of eight orders of magnitude.

Two parameters might enable microorganisms to achieve a higher MSP than larger organisms: temperature and size. Temperature affects the metabolic rates of organisms (32, 33) and some microorganisms are capable of growth at much higher temperatures than plants and animals. Notably, some of the highest MSP values in our dataset are for thermophiles such as *Geobacillus* LC300 at 72 °C and *Methanobacterium thermoautotrophicum* at 65 °C, though not all thermophiles or hyperthermophiles exhibit comparably high MSPs. However, normalizing all values in the dataset to 25 °C still leaves a >10-fold difference between the highest MSP in microorganisms vs. animals. A second parameter is size. Substrate mass transport limitations can restrict the metabolic rates of larger organisms, even at scales of 10's of μm (34). In contrast, molecular diffusion is sufficiently rapid at the μm- and sub-μm scales of prokaryotes that transport limitations are reduced or eliminated (35), a marked difference between prokaryotes and larger multicellular organisms such as animals and plants. At micron sizes, prokaryotic cells instead become limited by biochemical constraints, such as enzyme kinetic properties (36). Considering only biochemical constraints, a simple reference calculation[†] suggests a practical upper limit for MSP in the range of a few hundred W (g C)$^{-1}$. For comparison, the highest MSP in our dataset is 61 W (g C)$^{-1}$, for the aerobic, glucose-oxidizing, thermophilic bacterium *Geobacillus* LC300. Among anaerobes, the highest MSP we calculate is 22 W (g C)$^{-1}$, for the thermophilic archaeon *Methanobacterium thermoautotrophicum*[‡].

At the biosphere level, the highest MSP, 2.3 W (g C)$^{-1}$, is expressed by marine primary producers that sustain high specific growth rates (global average: 88 y^{-1}) likely driven by intense grazing pressure (22). Such high specific growth rates and high MSP can likely be sustained only in microbe-dominated communities. Hatton et al. (37) showed that, for organisms ranging from protists to mammals, the maximum rate of biomass production (Y, in g biomass y^{-1}), including both somatic growth and offspring production, scales with body mass (X, in g biomass) to the ¾ power: $Y = 3.5(X)^{0.75}$. This relationship predicts that high specific growth rates on the order of 100 y^{-1} are only achievable for organisms less massive than ~1 μg, and realistically smaller still under environmental conditions that do not support maximum growth rates. The observed carbon biomass of microalgae is of the order 10^{-6} to 10^{-2} μg (Dataset S1).

A lower biochemical bound on MSP is presumably set by the power required to sustain metabolic viability by maintaining a necessary complement of biomolecules against damage and maintaining a membrane potential against leakage (38, 39). Protein turnover is likely the dominant contributor to basal power requirements among cells of a few microns and smaller (30, 40), so conditions that minimize protein turnover and/or lower the cost of protein repair will favor low MSP. Taking amino acid racemization (i.e., spontaneous conversion from L- to D-form) to impose a lower bound on the necessary rate of protein repair or replacement, Lever et al. (30) calculated an energy cost equivalent to 4×10^{-9} to 4×10^{-7} W (g C)$^{-1}$ at 5 °C—assuming either complete protein replacement (upper value) or single amino acid repair (lower value). The genes required for single amino acid repair are widespread among deep sediment organisms (41), suggesting that

[†]A hypothetical microorganism that devotes 1% of dry biomass (~2% of protein mass) to a rate-limiting catabolic enzyme with a molecular weight of 30 kDa, a turnover number of k_{cat} = 50 s^{-1}, and a catabolic yield of −3,000 kJ (mol substrate)$^{-1}$ will realize an MSP of 100 W (g C)$^{-1}$ under kinetically saturating substrate concentrations. Allowing for variations in the dedicated enzyme mass fraction and k_{cat} suggests a practical upper limit MSP in the range of perhaps a few hundred W (g C)$^{-1}$. For reference, the weighted average bacterial protein molecular weight is 33 kDa (80), the median k_{cat} in an analysis of 78 enzymes involved in primary carbohydrate and energy metabolism was 79 s^{-1} (81), and the standard Gibbs energy change for aerobic glucose oxidation is −2,870 kJ (mol glucose)$^{-1}$. A 2% protein mass fraction is on par with the most abundant individual enzymes in *M. pneumonia, Escherichia coli*, and *S. cerevisiae* (82).

[‡]Some hyperthermophilic methanogens have doubling times as much as fivefold shorter than those of *M. thermoautotrophicum* (83), meaning that MSP in these organisms could be higher by a comparable factor (potentially >100 W (g C)$^{-1}$) if they operate at similar growth yield.

the lower range calculated by Lever et al. (30) might be more applicable.

At the biosphere level, the lowest average MSP, 2×10^{-5} W (g C)$^{-1}$, is associated with marine sediments >0.1 m below seafloor. There, cold, anoxia, and conditions that are static over thousands to millions of years favor extremely low rates of biomass turnover. Cold and anoxia lower rates of molecular damage (30), and the energetic cost of biosynthesis is lower under anoxic conditions (30, 42). Permanent anoxia also largely eliminates grazing pressure from animals, though viral lysis persists (43). Finally, environmentally static conditions may reduce the need for energetically costly regulation of protein synthesis. Sediments of the Peru Margin exemplify the potential for extreme reduction in biomass carbon turnover under such conditions. There, in sediments 1 to 40 meters below seafloor, biomass carbon turnover rates are 0.0002 to 0.005 y^{-1} (44)—nearly a million-fold lower than those of marine primary producers. On a global basis, the collective effects of cold, anoxic, and static conditions in sediments deeper than 0.1 m yield an average MSP nearly 70-fold lower than that in the immediately overlying (0 to 0.1 m) sediments, in which O_2 is present to varying degrees. This is nevertheless still 2 to 4 orders of magnitude higher than the racemization-based, theoretical lower limit calculated by Lever et al. (30).

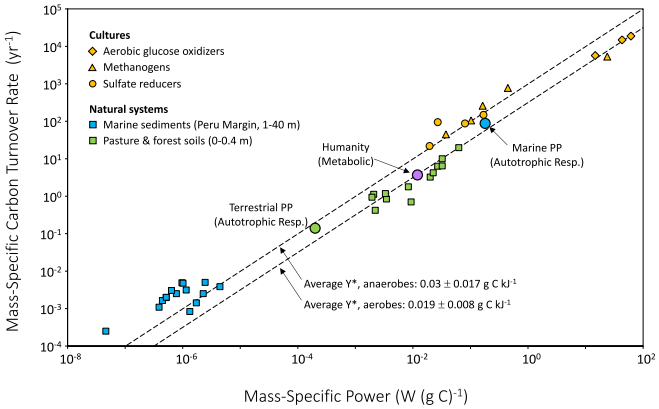

Fig. 3. Mass-specific carbon turnover rate, μ*, vs. mass specific power, MSP, for a range of populations and environments. Diagonal dashed lines denote average biosynthesis yield (Y*) in diverse cultures of heterotrophic microorganisms growing aerobically (*Lower* line) or anaerobically (*Upper* line) on a range of substrates (46). data: cultures: aerobic glucose oxidizers: (50)–(52); methanogens: (47), (53); sulfate reducers: (54), (55). Pasture and forest soils: (56). Marine sediments: (44). Marine primary producers: (22); terrestrial primary producers: (57). Humans: (58). *SI Appendix*, section 4.1 provides further details on the source data and calculations.

Biomass Carbon Turnover and MSP. The extremes in biosphere-level MSP are associated with corresponding extremes in biomass carbon turnover rates—very high for marine primary producers and very low for deep marine sediments—suggesting that the two quantities may be correlated. However, multiple energy-requiring processes besides biosynthesis (which sustains biomass carbon turnover) can demand a share of MSP, making it uncertain whether MSP and biomass carbon turnover will be tightly correlated over a large range. We assessed the extent of correlation between MSP and biomass carbon turnover rate by comparing multiple systems, spanning many orders of magnitude in MSP, for which both quantities have been measured.

The term "biomass carbon turnover" acknowledges that biosynthesis occurs, at an energetic cost, even when biomass does not increase. In a nongrowing or slowly growing individual, this may encompass turnover of molecules and cells (45); it can also encompass turnover of individuals in a population at steady state (i.e., a population in which biomass remains constant). For comparison to MSP, we consider the biomass carbon turnover rate on a mass-specific basis. The resulting "specific carbon turnover rate", μ*, is analogous to the specific growth rate, μ, but considers total carbon turnover rather than net growth. Like μ, μ* has units of grams carbon biomass synthesized per gram standing carbon biomass per time, which reduce to reciprocal time (e.g., s^{-1}). Dividing μ* (units: (g C biosynthesis) × s^{-1} × (g C biomass)$^{-1}$) by MSP (units: J × s^{-1} × (g C biomass)$^{-1}$) gives a quantity with units of g C biosynthesis per Joule (g C J^{-1}), which we refer to as the biosynthesis yield, Y*. (We subsequently express μ* in units of y^{-1} and Y* in units of g C kJ^{-1}.) Y* is analogous to the growth yield, Y, a quantity commonly used in microbiology to relate a net increase in biomass to an amount of substrate consumed, but Y* is distinct in two regards. First, Y* refers to carbon turnover, rather than net growth, in order to include the energy spent on biosynthesis in systems with little or no net change in biomass[§]. Second, Y* relates carbon turnover to energy utilization rather than substrate consumption, in order to provide a common energetic basis for comparing organisms that use different or mixed substrates (46).

Fig. 3 plots μ* against MSP for a range of systems in which both quantities have been independently determined and shows that they remain correlated over 8+ orders of magnitude. A perfect correlation between μ* and MSP would plot on Fig. 3 as a straight line that represents a constant value of Y*. Divergence from perfect correlation (equivalent to variations in Y*) could result from variations in i) the thermodynamic efficiency of catabolic energy conservation (the fraction of the catabolic energy liberation that is captured vs. lost to heat), ii) the energetic cost of biosynthesis, and iii) the fraction of metabolic energy that is dedicated to biosynthesis vs. other expenditures. Of these three factors, the fractional allocation of energy to biosynthesis (iii) has the potential to vary most over a large range in MSP because, if a fixed set of nonsynthesis maintenance costs must be met, the energy left to fuel biosynthesis would diminish, potentially to zero, as MSP declines. It is evident that *total* maintenance costs—encompassing both synthesis and nonsynthesis costs—do not remain fixed as substrate consumption rates drop (e.g., refs. 47 and 48). However, any nonsynthesis costs that are obligate, such as maintaining energized membranes (e.g., ref. 49), could potentially come to dominate the cellular energy budget at low MSP, and therefore drive Y* to low values. The strong correlation exhibited in Fig. 3 across the entire range indicates that the fractional allocation of MSP to carbon turnover does not decrease dramatically, even as MSP changes over nearly nine orders of magnitude. Rather, soils and aerobic glucose–oxidizing cultures, which collectively span 4.5 orders of magnitude in MSP, both fall close to the mean value of Y* (0.019 ± 0.008 g C kJ^{-1}; lower dashed line in Fig. 3) measured in diverse cultures of aerobic heterotrophic microorganisms growing on a range of substrates (46). Similarly, anoxic marine sediments and cultures of sulfate-reducing bacteria and methanogenic archaea, which span an even larger range, fall close to the mean value of Y* (0.03 ± 0.017 g C kJ^{-1}; upper dashed line in Fig. 3) measured for anaerobes grown on a range of substrates (46).

To the extent that the correlation in Fig. 3 is broadly applicable, our estimates of MSP in the various components of the biosphere can constrain the rates of biomass carbon turnover in those

[§]We note that, for the cultures in Fig. 3, specific growth rate is plotted rather than specific carbon turnover rate. While this represents a lower limit on specific carbon turnover rate, we consider it a close approximation. For example, in the case of the methanogen culture with the lowest MSP in Fig. 3, growing at 1% of its maximum rate, net growth still accounted for >70% of total energy utilization (47), suggesting that specific growth rate likely did not underestimate specific carbon turnover rate by more than ~30%.

environments. This notion is supported by the strong correlation exhibited when our estimates of MSP are plotted vs. independent measures of protein carbon turnover rate in humans (58), global average specific growth rate for marine primary producers (22), and global average biomass carbon turnover rate for terrestrial primary producers (57). A similar approach can be applied to the components of the biosphere for which, to our knowledge, independent estimates of biomass carbon turnover have not yet been made. Using $Y^* = 0.025$ g C kJ^{-1}—midway between the culture-based means for aerobic and anaerobic heterotrophs (diagonal dashed lines), and approximating the value exhibited by humans and marine and terrestrial primary producers (Fig. 3)—gives specific biomass carbon turnover rates of ~2.3 y^{-1} for terrestrial soil microbes, ~8.5 y^{-1} for the marine water column, and ~1.0 y^{-1} and ~0.01 y^{-1} for marine sediments at 0 to 0.1 m and >0.1 m depth, respectively. Considering the high μ^* of the global phytoplankton community (88 y^{-1}; (22))), the components of the marine biosphere thus exhibit a systematic, four order of magnitude decrease in specific biomass carbon turnover rate, from the sunlit surface ocean to the deep sediments beneath.

Convergence in MSP? It is remarkable that the global biosphere MSP, and that of terrestrial primary producers (by the measure of photon capture), soil biota, marine pelagic biota, humanity, livestock, and more than two-thirds of the species-level MSP measurements all fall within 6-fold of the all-species mean (Fig. 2), despite an overall range in basal MSP among individual species of five orders of magnitude, and as much as eight orders of magnitude when considering maximum and deep sediment MSP. An earlier study posited that MSP clusters around a "metabolic optimum" as a result of "natural selection of organismal designs that fit within a narrow range of MSP" (2). Could the seeming convergence in organism- and biosphere-level MSP reflect such an effect? While metabolism itself is not a unit of selection but, rather, the realized sum of anabolic and catabolic reactions that are individually under selection, several factors could contribute to the observed convergence in MSP.

The literature surrounding MSP is dominated by measurements made on animal species, particularly mammals, birds, insects, and fishes. Even within these groups, studies have focused primarily on animals that are amenable to respirometric studies, such as domesticated species (livestock), small or docile wild animals, and primates including humans (59). There are fewer data on plants, microorganisms, larger wild animals, animals from polar regions, marine animals, and especially marine animals whose habitat (e.g., the deep sea) and morphology (e.g., gelatinous plankton) make such measurements challenging. Our dataset reflects this bias, such that the mean MSP of 0.012 W $(g\ C)^{-1}$ is determined largely by a heavily represented group of animals with shared attributes. Convergence toward the mean in our dataset thus effectively implies convergence toward the MSP of this core group of organisms.

For all organisms, MSP is governed by both intrinsic factors (e.g., maintenance, reproduction, damage repair, allometric scaling) and environmental factors (e.g., temperature, food availability, ecological interactions), but the balance between the two may vary. Relative to microorganisms, multicellular organisms are more capable of modulating MSP during short-term variations in environmental conditions through intrinsic factors, such as mobilizing nutrient stores or hormonal depression of metabolism (60, 61). Studies have also suggested that MSP is set by a "biological pacemaker" that could, in principle, serve as an MSP "setpoint" for animals [(62), (63) and references therein], though there is no broad consensus that such a system exists. Combined with the factors that may limit animal and plant MSP to a narrower range than in microorganisms (see "The Range in MSP"), these considerations could contribute to convergence in animal MSP. In this light, it is reasonable, if not unsurprising, to find that the calculated MSP of humanity and livestock—as members of the "common core" of heavily studied organisms—both agree closely with the all-species mean. But what of a broader biosphere dominated by plants and microorganisms which, as groups relatively less represented in the organism-level data, do not heavily influence the all-species mean?

The MSP of the global biosphere is effectively set by primary producers, which account for almost 100% of global energy capture and 90% of global biomass (Table 1). For that group, similarity to the all-species mean occurs only with the "photon capture" measure of energy utilization. By the measure of autotrophic respiration—which places the comparison between autotrophs and heterotrophs on a more equivalent basis—MSP among terrestrial primary producers falls 30-fold below the all-species mean when considering all plant biomass and 10-fold below when considering active plant tissues only (Table 1).

In the case of soil and marine water column biota, agreement with the all-species mean MSP is likely a fortuitous result of averaging across a large continuum of metabolic states rather than a convergence based on physiological commonalities. Whereas MSP in the common core of heavily studied organisms may be strongly influenced by intrinsic physiological factors, that of microorganisms—the dominant biota in both soils and the marine water column—is heavily dependent on environmental context. Microbe-dominated marine sediments provide a clear example of this. There, high spatial resolution measurements made over the upper meter of sediments demonstrate that MSP diminishes in continuous fashion over a more than five order of magnitude range, as bulk energy availability diminishes in parallel (Fig. 4). Averaging across such a depth series will yield a single intermediate MSP value that does not reflect convergence toward an intrinsic physiological optimum but, rather, the bulk behavior of organisms

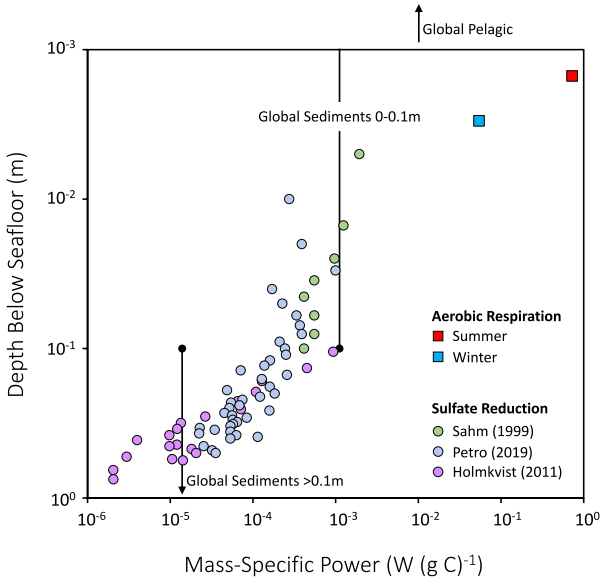

Fig. 4. MSP vs. depth in marine sediments from Aarhus Bay, Denmark. Squares: MSP associated with aerobic respiration of organic carbon during the summer (red) and winter (blue). Circles: MSP associated with sulfate-based respiration of organic matter compiled from three studies. Vertical lines denote the global MSP estimates for marine heterotrophs in the water column ("Global pelagic") and 0 to 0.1 m and >0.1 m sediment layers. MSP is calculated from cell-specific sulfate reduction rates reported in refs. 64–66 and from O_2 uptake measurements reported in ref. 67 (*SI Appendix*, section 4.2).

whose MSP is driven primarily by environmental factors. This same effect is seemingly at work across the full span of the microbe-dominated marine biosphere, where systematically diminishing energy availability from sunlit ocean surface to deep sediment biosphere is accompanied by a five order of magnitude change in MSP but little change in biomass (Fig. 2).

Humanity. From a purely biological perspective, humanity's MSP is unremarkable. Our 0.012 W $(g\ C)^{-1}$ is comparable to the average for marine water column biota and the organism-level mean and lies within ~twofold of the MSP of the biosphere overall. However, when factoring in our use of energy in technological terms—which, as with biological consumption, is inherently tied to the carbon cycle—our MSP increases 18-fold. The increase is greater still in heavily industrialized regions. For example, the MSP of the US population, when considering both biological and technological consumption of energy, is 0.52 W $(g\ C)^{-1}$—equivalent to that of a sprinting antelope [*Antilocapra americana*: 0.52 W $(g\ C)^{-1}$; Dataset S1]. This far exceeds MSP in any of the biosphere components we considered, with the exception of marine primary producers [2.3 W $(g\ C)^{-1}$], whose high MSP is sustainable only by virtue of a population turnover time of a few days. Humanity has also impacted the MSP of the biosphere as a whole, by nearly doubling turnover rates of vegetation biomass carbon stock through land use and land management changes (57). By virtue of such changes, Earth presently contains less than half the plant biomass that could otherwise be sustained under the present climate regime (17). However, NPP (equivalent to net biosynthesis rate) remains at 90% of its potential value in the absence of human-induced change (68). The implication is that humanity has nearly doubled the mass-specific metabolic rate of Earth's biosphere, despite comprising less than 0.02% of its mass.

Conclusions

Earth's biosphere has an overall "metabolic rate" of 0.005 W $(g\ C)^{-1}$, which is set by plants and microbial primary producers, and by the impact of humanity upon those populations. Across the diversity of microbial taxa, MSP ranges over eight orders of magnitude or more, and the microbe-dominated components of the marine biosphere span fully five of those orders of magnitude. The upper and lower extremes in biosphere-level MSP are driven by a 20,000-fold difference in energy flux and differing ecological niches that yield extremely high and low rates of biomass carbon turnover. Indeed, biomass carbon turnover rate is correlated with MSP across 8 orders of magnitude and, based on our estimates of MSP, this correlation predicts global biomass carbon turnover rates of ~2.3 y^{-1} for terrestrial soil biota, ~8.5 y^{-1} for marine water column biota, and ~1.0 y^{-1} and ~0.01 y^{-1} for marine sediment biota in the 0 to 0.1 m and >0.1 m depth intervals, respectively. Despite the very large range in MSP that is both physiologically possible and is expressed at the biosphere level, the MSP of the global biosphere, terrestrial primary producers (by the measure of photon capture), soil biota, marine water column biota, humanity, livestock, and more than two-thirds of the organism-level MSP measurements all fall within sixfold of the all-species mean. This seeming convergence is in some cases potentially a result of organisms having shared physiological determinants of MSP but, in the microbe-dominated components of the biosphere, is a fortuitous result of averaging across a large continuum of environmental MSP.

Materials and Methods

Mass and Power of Organisms. All organism-level metabolic rates and masses were compiled from the literature sources in *SI Appendix*, Table S1 and are included in Dataset S1, which specifies: a) genus/species of organism, b) individual/mean body mass, c) individual/mean metabolic rate, and d) literature reference. Taxonomy was generally assigned according to the Integrated Taxonomic Information system (ITIS; www.itis.gov) and is specified with a taxonomic serial number (tsn) unique for the associated scientific name. Conversion between dry biomass and carbon biomass assumes a 2:1 ratio unless otherwise specified, while conversion between wet mass and dry mass is taxon specific, as specified in Dataset S1. Metabolic rates are converted from O_2 consumption rates to Watts using a factor of 20 J mL^{-1} O_2, which is a mean of published values (2). The temperature normalization calculation uses taxon-specific conversion factors (Q_{10}) as described in *SI Appendix*.

Mass and Power at the Biosphere Level.

Mass estimates. With the exception of humanity and marine consumers in sediments, 0 to 0.1m, all mass estimates are taken from the literature cited in Table 1. The methodology for estimating the masses of humanity and marine sediments (0 to 0.1m) is discussed in detail in *SI Appendix* and summarized briefly below:

Humanity. We base our estimate on the UN-FAO global population estimate of 8.0 billion in late 2022 and an estimated average human carbon mass of 11 ± 5 kg C. The latter number is based on an all-ages average carbon mass for the US population of 17.3 kg C (69), scaled down to account for differences in mass and other factors in the global vs. US populations [(70); see *SI Appendix*].

Marine sediments (0 to 0.1m). The mass estimate is based on a mean microbial cell abundance of 1.3×10^{14} cells m^{-2} in the bioturbated upper layer of the global seabed (71) and an average cell carbon mass of 23 fg C for cells in the 0 to 0.1 m interval (72). This estimate does not include contributions from seabed animals or sediments underlying ocean gyres, which we find to be negligible (*SI Appendix*, section 2).

Power estimates. Power estimates are based on published global chemical (primarily carbon) fluxes using the relations and energy conversion factors described below. The rationale underlying the choice of flux estimates and energy conversion factors is discussed in detail in *SI Appendix*.

Marine Primary Producers (Photon Capture): $P_{photon\text{-}marine} = NPP_{marine} * (1/\varphi_{max\text{-}marine}) * E_{photon}$

NPP_{marine}, the global NPP attributable to marine phototrophs, is (1.38 ± 0.1) × 10^8 mol C s^{-1}, converted from 52.1 ± 3.8 Pg C y^{-1} (22); $\phi_{max\text{-}marine}$, the maximum quantum yield of net carbon fixation (73), is 0.025 ± 0.002 mol C (mol photons)$^{-1}$ (22); and E_{photon}, the spectrum-weighted mean energy of photons in the PAR portion of the visible light spectrum, is 2.1×10^5 J (mol photons)$^{-1}$ [converted from 2.77×10^{21} quanta s^{-1} kW^{-1}; (74)].

Marine Primary Producers (Autotrophic Respiration): $P_{AR\text{-}marine} = -\Delta G_{AR} * (GPP_{marine} - NPP_{marine})$

ΔG_{AR}, the Gibbs energy change associated with autotrophic respiration, is -4.74×10^5 J (mol C)$^{-1}$; GPP_{marine}, the global GPP attributable to marine phototrophs, is (3.4 ± 0.4) × 10^8 mol C s^{-1}, based on a range of 103 to 150 Pg C y^{-1} (21); and NPP_{marine} is as above.

Terrestrial Primary Producers (Photon Capture): $P_{photon\text{-}terr} = GPP_{terrestrial} * (1/\varphi_{max\text{-}terrestrial}) * E_{photon}$

$GPP_{terrestrial}$, the global GPP attributable to terrestrial phototrophs, is (3.0 to 5.0) × 10^8 mol C s^{-1}, converted from 115 to 190 Pg C y^{-1} for the period 1982 to 2016 (20, 75); $\varphi_{max\text{-}terrestrial}$, the maximum quantum yield of gross carbon fixation, is 0.053 ± 0.003 mol C (mol photons)$^{-1}$ (based on data in ref. 73); and E_{photon} is as above.

Terrestrial Primary Producers (Autotrophic Respiration): $P_{AR\text{-}terr} = -\Delta G_{AR} * R_{AR}$

R_{AR}, a direct estimate of the global rate of autotrophic respiration in terrestrial phototrophs, is (1.7 ± 0.3) × 10^8 mol C s^{-1}, converted from 64 ± 12 Pg C y^{-1} (76); ΔG_{AR} is as above.

Marine Consumers (Pelagic): $P_{HR\text{-}pelagic} = -\Delta G_{MC} * (NPP_{marine} - J_{C\text{-}benthic})$

ΔG_{MC}, the Gibbs energy change associated with aerobic respiration of marine organic matter, is -4.43 × 10^5 J (mol C)$^{-1}$; $J_{C\text{-}benthic}$, the globally integrated flux of particulate organic carbon to the seabed, is estimated at (7.9 ± 1.9) × 10^6 mol C·s^{-1} (*SI Appendix*, section 3.2); and NPP_{marine} is as above.

Marine Heterotrophic Consumers (Sediments, 0-0.1 m): $P_{HR\text{-}seds(0\ to\ 0.1)} = -\Delta G_{MC} * R_{C\text{-}aerobic}$

$R_{C\text{-}aerobic}$, the globally integrated rate of aerobic respiration of carbon in the seabed, is, 6.7 ± 1.7 × 10^6 mol C s^{-1}, converted from 212 ± 55 Tmol C y^{-1} (77); and ΔG_{MC} is as above. We find that the power associated with both anaerobic respiration of carbon within the 0 to 0.1m sediment interval and aerobic respiration

in sediments deeper than 0.1 m is negligible in relation to the power associated with aerobic respiration in the 0 to 0.1m interval (*SI Appendix*, section 3.2).

Marine Heterotrophic Consumers (Sediments >0.1 m): $P_{HR\text{-}seds(>0.1\ m)} = (-\Delta G_{MC} * R_{C\text{-}deep/aerobic}) + (-\Delta G_{MC\text{-}SO4} * R_{C\text{-}deep/sulfate}) + (-\Delta G_{SR} * 0.125 * R_{deep/radiolysis})$

This formulation recognizes that both aerobic and sulfate-based respiration of organic carbon and respiration based on oxidants and reductants produced by water radiolysis contributes to the power associated with deep sediment populations. Here, $R_{C\text{-}deep/aerobic}$, the globally integrated rate of aerobic carbon respiration in sediments deeper than 0.1m, is 1.43×10^5 mol C s^{-1} (estimated as a fraction of the global subseafloor aerobic respiration of 18 Tg C y^{-1} reported by ref. (31); see *SI Appendix*); $R_{C\text{-}deep/sulfate}$, the globally integrated rate of sulfate-based carbon respiration in sediments deeper than 0.1 m, is 1.94×10^6 mol C s^{-1} [estimated as a fraction of the global seabed sulfate reduction rate of 45 Tmol S y^{-1} (78); see *SI Appendix*, section 3.2]; $R_{deep/radiolysis}$, the globally integrated rate of radiolytic reductant production in sediments deeper than 0.1 m, is 8.6×10^5 mol electron equivalents per second, and the coefficient of that term (0.125) accounts for the 1:8 stoichiometry of electron equivalents to sulfate in the complete reduction of sulfate to sulfide (79); ΔG_{MC} is as above; $\Delta G_{MC\text{-}SO4}$, the Gibbs energy change associated with sulfate-based respiration of marine organic matter, is -3.22×10^4 J (mol C)$^{-1}$; and ΔG_{SR}, the Gibbs energy change associated with sulfate reduction, is -2.74×10^4 J (mol SO_4^{2-})$^{-1}$.

Terrestrial Heterotrophic Consumers (Soils 0-8 m): $P_{HR\text{-}soils} = -\Delta G_{TC} * R_{HR}$

Here, ΔG_{TC}, the Gibbs energy change associated with aerobic respiration of terrestrial organic matter, is -4.83×10^5 J (mol C)$^{-1}$; and R_{HR}, the global rate of heterotrophic respiration in soils, is $(1.03 \pm 0.26) \times 10^8$ mol C s^{-1}, based on a direct estimate of 39 Pg C y^{-1} with an interquartile range of 33 to 46 Pg C y^{-1} (24).

Geochemical energy sources. The flux of energy potentially available to chemolithoautotrophic microorganisms from geochemical sources was compiled from published estimates of the fluxes of H_2, H_2S, CH_4, and Fe^{2+} (*SI Appendix*, Table S5)–representing reductants that can be biologically utilized and have fluxes that are significant in magnitude. Upper limits on the energy available from these fluxes were computed by assuming complete consumption via aerobic respiration, with associated Gibbs energy changes computed by assuming electron donor and O_2 concentrations of 100 μmol kg^{-1} and 100 nmol O_2 kg^{-1}, respectively, at 25 °C and pH 7 (*SI Appendix*, section 3.3). A summary of the resulting potential energy supplies, broken down by environment and electron donor, is given in *SI Appendix*, Table S4.

Data, Materials, and Software Availability. All study data are included in the article and/or supporting information.

ACKNOWLEDGMENTS. This work was supported by NASA Grant 80NSSC19K1427 (T.M.H. and P.R.G.), the NASA Planetary Science Division ISFM Program (T.M.H.), NSF Grant 1816652 (T.M.M.), and NASA's Virtual Planetary Laboratory under NASA Astrobiology Institute Cooperative Agreement Number NNA13AA93A and Grant Number 80NSSC18K0829. We are grateful to Mike Behrenfeld, Hans Røy, Doug LaRowe, James Bradley, Jens Kallmeyer, and Tristan Caro for helpful discussions. We acknowledge Bar-On et al. (2018), whose work both inspired and enabled the conduct of the present study.

1. K. A. Nagy, I. A. Girard, T. K. Brown, Energetics of free-ranging mammals, reptiles, and birds. *Annu. Rev. Nutr.* **19**, 247–277 (1999).
2. A. M. Makarieva *et al.*, Mean mass-specific metabolic rates are strikingly similar across life's major domains: Evidence for life's metabolic optimum. *Proc. Natl. Acad. Sci. U.S.A.* **105**, 16994–16999 (2008).
3. V. M. Savage *et al.*, The predominance of quarter-power scaling in biology. *Funct. Ecol.* **18**, 257–282 (2004).
4. A. M. Makarieva, V. G. Gorshkov, B.-L. Li, Energetics of the smallest: Do bacteria breathe at the same rate as whales? *Proc. Biol. Sci.* **272**, 2219–2224 (2005).
5. L. N. Hudson, N. J. B. Isaac, D. C. Reuman, The relationship between body mass and field metabolic rate among individual birds and mammals. *J. Anim. Ecol.* **82**, 1009–1020 (2013).
6. J. F. Gillooly, J. P. Gomez, E. V. Mavrodiev, A broad-scale comparison of aerobic activity levels in vertebrates: endotherms versus ectotherms. *Proc. Biol. Sci.* **284**, 20162328 (2017).
7. J. G. Rubalcaba, W. C. E. P. Verberk, A. J. Hendriks, B. Saris, H. A. Woods, Oxygen limitation may affect the temperature and size dependence of metabolism in aquatic ectotherms. *Proc. Natl. Acad. Sci. U.S.A.* **117**, 31963–3196 (2020).
8. B. K. McNab, On the utility of uniformity in the definition of basal rate of metabolism. *Physiol. Zool.* **70**, 718–720 (1997).
9. E. A. Dawes, E. W. Ribbons, The endogenous metabolism of microorganisms. *Ann. Rev. Microbiol.* **16**, 241–264 (1962).
10. P. J. Butler, J. A. Green, I. L. Boyd, J. R. Speakman, Measuring metabolic rate in the field: The pros and cons of the doubly labelled water and heart rate methods. *Funct. Ecol.* **18**, 168–183 (2004).
11. V. M. Savage *et al.*, The predominance of quarter-power scaling in biology. *Funct. Ecol.* **18**, 257–282 (2004).
12. A. E. McKechnie, R. P. Freckleton, W. Jetz, Phenotypic plasticity in the scaling of avian basal metabolic rate. *Proc. Biol. Sci.* **273**, 931–937 (2006).
13. J. E. Niven, J. P. Scharlemann, Do insect metabolic rates at rest and during flight scale with body mass? *Biol. Lett.* **1**, 346–349 (2005).
14. Y. M. Bar-On, R. Phillips, R. Milo, The biomass distribution on Earth. *Proc. Natl. Acad. Sci. U.S.A.* **115**, 6506–6511 (2018).
15. I. A. Hatton, R. F. Heneghan, Y. M. Bar-On, E. D. Galbraith, The global ocean size spectrum from bacteria to whales. *Sci. Adv.* **7**, eabh3732 (2021).
16. J. Kallmeyer, R. Pockalny, R. R. Adhikari, D. C. Smith, S. D'Hondt, Global distribution of microbial abundance and biomass in subseafloor sediment. *Proc. Natl. Acad. Sci. U.S.A.* **109**, 16213–16216 (2012).
17. K. H. Erb *et al.*, Unexpectedly large impact of forest management and grazing on global vegetation biomass. *Nature* **553**, 73–76 (2018).
18. C. Magnabosco *et al.*, The biomass and biodiversity of the continental subsurface. *Nat. Geosci.* **11**, 707–717 (2018).
19. British Petroleum Corporation, *Statistical Review of World Energy* (ed. 69th, British Petroleum Corporation, 2020).
20. D. Crisp *et al.*, How well do we understand the land-ocean-atmosphere carbon cycle?. *Rev. Geophys.* **60**, e2021RG000736 (2022).
21. Y. Huang, D. Nicholson, B. Huang, N. Cassar, Global estimates of marine gross primary production based on machine learning upscaling of field observations. *Global Biogeochem. Cycles* **35**, e2020GB006718 (2021).
22. G. M. Silsbe, M. J. Behrenfeld, K. H. Halsey, A. J. Milligan, T. K. Westberry, The CAFE model: A net production model for global ocean phytoplankton. *Global Biogeochem. Cycles* **30**, 1756–1777 (2016).
23. L. Gómez-Consarnau *et al.*, Microbial rhodopsins are major contributors to the solar energy captured in the sea. *Sci. Adv.* **5**, eaaw8855 (2019).
24. P. Ciais *et al.*, Empirical estimates of regional carbon budgets imply reduced global soil heterotrophic respiration. *Nat. Sci. Rev.* **8**, nwaa145 (2021).
25. P. A. Srere, "Organization of proteins within the mitochondrion" in *Organized Multienzyme Systems: Catalytic Properties*, G. R. Welch, Ed. (Academic Press, 1985), pp. 1-65.
26. R. K. Suarez, Hummingbird flight: sustaining the highest mass-specific metabolic rates among vertebrates. *Experientia* **48**, 565–570 (1992).
27. M. C. McCarthy, B. J. Enquist, Organismal size, metabolism and the evolution of complexity in metazoans. *Evol. Ecol. Res.* **7**, 681–696 (2005).
28. T. M. Hoehler, B. B. Jørgensen, Microbial life under extreme energy limitation. *Nat. Rev. Microbiol.* **11**, 83–94 (2013).
29. D. E. LaRowe, J. P. Amend, Power limits for microbial life. *Front. Microbiol.* **6**, 718 (2015).
30. M. A. Lever *et al.*, Microbial life under extreme energy limitation: A synthesis of laboratory- and field-based investigations. *FEMS Microbiol. Rev.* **39**, 688–728 (2015).
31. J. A. Bradley *et al.*, Widespread energy limitation to life in global subseafloor sediments. *Sci. Adv.* **6**, eaba0697 (2020).
32. J. F. Gillooly, J. H. Brown, G. B. West, V. M. Savage, E. L. Charnov, Effects of size and temperature on metabolic rate. *Science* **293**, 2248–2251 (2001).
33. A. Clarke, H. O. Pörtner, Temperature, metabolic power and the evolution of endothermy. *Biol. Rev.* **85**, 703–727 (2010).
34. U. Riebesell, D. A. Wolf-Gladrow, V. Smetacek, Carbon dioxide limitation of marine phytoplankton growth rates. *Nature* **361**, 249–251 (1993).
35. H. N. Schulz, B. B. Jørgensen, Big bacteria. *Annu. Rev. Microbiol.* **55**, 105–137 (2001).
36. L. Li, G. Wang, Enzymatic origin and various curvatures of metabolic scaling in microbes. *Sci. Rep.* **9**, 4082 (2019).
37. I. A. Hatton *et al.*, The predator-prey power law: Biomass scaling across terrestrial and aquatic biomes. *Science* **349**, aac6284 (2015).
38. R. Y. Morita, *Bacteria in Oligotrophic Environments* (Chapman & Hall, New York, 1997), p. 529.
39. J. D. Keene, RNA regulons: Coordination of post-transcriptional events. *Nat. Rev. Genet.* **8**, 533–543 (2007).
40. C. P. Kempes *et al.*, Drivers of bacterial maintenance and minimal energy requirements. *Front. Microbiol.* **8**, 31 (2017).
41. S. S. Mhatre *et al.*, Microbial biomass turnover times and clues to cellular protein repair in energy-limited deep Baltic Sea sediments. *FEMS Microbiol. Ecol.* **95**, fiz068 (2019).
42. T. M. McCollom, J. P. Amend, A thermodynamic assessment of energy requirements for biomass synthesis by chemolithoautotrophic micro-organisms in oxic and anoxic environments. *Geobiology* **3**, 135–144 (2005).
43. L. Cai *et al.*, Active and diverse viruses persist in the deep sub-seafloor sediments over thousands of years. *ISME J.* **13**, 1857–1864 (2019).
44. B. A. Lomstein, A. T. Langerhuus, S. D'Hondt, B. B. Jørgensen, A. J. Spivack, Endospore abundance, microbial growth and necromass turnover in deep sub-seafloor sediment. *Nature* **484**, 101–104 (2012).
45. R. Sender, R. Milo, The distribution of cellular turnover in the human body. *Nat. Med.* **27**, 45–48 (2021).
46. J. J. Heijnen, J. P. van Dijken, In search of a thermodynamic description of biomass yields for the chemotrophic growth of microorganisms. *Biotechnol. Bioeng.* **39**, 833–858 (1992).
47. A. L. Müller *et al.*, An alternative resource allocation strategy in the chemolithoautotrophic archaeon *Methanococcus maripaludis*. *Proc. Natl. Acad. Sci. U.S.A.* **118**, e2025854118 (2021).

48. D. A. Lipson, The complex relationship between microbial growth rate and yield and its implications for ecosystem processes. *Front. Microbiol.* **6**, 615 (2015).
49. J. L. C. M. van den Vossenberg, T. Ubbink-Kok, M. G. L. Elferink, A. J. M. Driessen, W. N. Konings, Ion permeability of the cytoplasmic membrane limits the maximum growth temperature of bacteria and archaea. *Mol. Microbiol.* **18**, 925–932 (1995).
50. L. G. Fuentes *et al.*, Modification of glucose import capacity in *Escherichia coli*: Physiologic consequences and utility for improving DNA vaccine production. *Microb. Cell Factory* **12**, 42 (2013).
51. L. T. Cordova, C. P. Long, K. P. Venkataramanan, M. R. Antoniewicz, Complete genome sequence, metabolic model construction and phenotypic characterization of *Geobacillus* LC300, an extremely thermophilic, fast growing, xylose-utilizing bacterium. *Metab. Eng.* **32**, 74–81 (2015).
52. C. P. Long, J. E. Gonzalez, R. M. Cipolla, M. R. Antoniewicz, Metabolism of the fast-growing bacterium *Vibrio natriegens* elucidated by ^{13}C metabolic flux analysis. *Metab. Eng.* **44**, 191–197 (2017).
53. P. Schönheit, J. Moll, R. K. Thauer, Growth parameters (K_S, m_{max}, Y_S) of *Methanobacterium thermoautotrophicum*. *Arch. Microbiol.* **127**, 59–65 (1980).
54. I. H. Tarpgaard, A. Boetius, K. Finster, Desulfobacter psychrotolerans sp. nov., a new psychrotolerant sulfate-reducing bacterium and descriptions of its physiological response to temperature changes. *Antonie Van Leeuwenhoek* **89**, 109–124 (2006).
55. A. Marietou, K. U. Kjeldsen, C. Glombitza, B. B. Jørgensen, Response to substrate limitation by a marine sulfate-reducing bacterium. *ISME J.* **16**, 200–210 (2022).
56. M. Spohn, K. Klaus, W. Wanek, A. Richter, A., Microbial carbon use efficiency and biomass turnover times depending on soil depth–Implications for carbon cycling. *Soil Biol. Biochem.* **96**, 74–81 (2016).
57. K. H. Erb *et al.*, Biomass turnover time in terrestrial ecosystems halved by land use. *Nat. Geosci.* **9**, 674–678 (2016).
58. S. Welle, K. S. Nair, Relationship of resting metabolic rate to body composition and protein turnover. *Am. J. Physiol.* **258**, E990–E998 (1990).
59. P. S. Agutter, D. N. Wheatley, Metabolic scaling: Consensus or controversy? *Theor. Biol. Med. Model.* **1**, 1–11 (2004).
60. J. Avaria-Llautureo, C. E. Hernández, E. Rodríguez-Serrano, C. Venditti, The decoupled nature of basal metabolic rate and body temperature in endotherm evolution. *Nature* **572**, 651–654 (2019).
61. A. C. I. Kiss, J. E. de Carvalho, C. A. Navas, F. R. Gomes, Seasonal metabolic changes in a year-round reproductively active subtropical tree-frog (Hypsiboas prasinus). *Comp. Biochem. Physiol. Part A Mol. Integr. Physiol.* **152**, 182–188 (2009).
62. A. J. Hulbert, P. L. Else, Mechanisms underlying the cost of living in animals. *Ann. Rev. Physiol.* **62**, 207–235 (2000).
63. D. S. Glazier, Is metabolic rate a universal 'pacemaker' for biological processes? *Biol. Rev.* **90**, 377–407 (2015).
64. K. Sahm, B. J. MacGregor, B. B. Jørgensen, D. A. Stahl, Sulphate reduction and vertical distribution of sulphate-reducing bacteria quantified by rRNA slot-blot hybridization in a coastal marine sediment. *Environ. Microbiol.* **1**, 65–74 (1999).
65. L. Holmkvist, T. G. Ferdelman, B. B. Jørgensen, A cryptic sulfur cycle driven by iron in the methane zone of marine sediment (Aarhus Bay, Denmark). *Geochim. Cosmochim. Acta* **75**, 3581–3599 (2011).
66. C. Petro *et al.*, Marine deep biosphere microbial communities assemble in near-surface sediments in Aarhus Bay. *Front. Microbiol.* **10**, 758 (2019).
67. H. Rasmussen, B. B. Jorgensen, Microelectrode studies of seasonal oxygen uptake in a coastal sediment role of molecular diffusion. *Mar. Ecol. Progr. Ser.* **81**, 289–303 (1992).
68. H. Haberl *et al.*, Quantifying and mapping the human appropriation of net primary production in earth's terrestrial ecosystems. *Proc. Natl. Acad. Sci. U.S.A.* **104**, 12942–12947 (2007).
69. T. O. West, G. Marland, N. Singh, B. L. Bhaduri, A. B. Roddy, The human carbon budget: An estimate of the spatial distribution of metabolic carbon consumption and release in the United States. *Biogeochemistry* **94**, 29–41 (2009).
70. S. C. Walpole *et al.*, The weight of nations: An estimation of adult human biomass. *BMC Publ. Health* **12**, 439 (2012).
71. M. A. Rex *et al.*, Global bathymetric patterns of standing stock and body size in the deep-sea benthos. *Mar. Ecol. Prog. Ser.* **317**, 1–8 (2006).
72. S. Braun *et al.*, Size and carbon content of sub-seafloor microbial cells at Landsort Deep, Baltic Sea. *Front. Microbiol.* **7**, 1375 (2016).
73. J. B. Skillman, Quantum yield variation across the three pathways of photosynthesis: Not yet out of the dark. *J. Exp. Bot.* **59**, 1647–1661 (2008).
74. A. Morel, R. C. Smith, Relation between total quanta and total energy for aquatic photosynthesis 1. *Limnol. Oceanogr.* **19**, 591–600 (1974).
75. W. Cai, I. C. Prentice, Recent trends in gross primary production and their drivers: Analysis and modelling at flux-site and global scales. *Environ. Res. Lett.* **15**, 124050 (2020).
76. A. Ito, Constraining size-dependence of vegetation respiration rates. *Sci. Rep.* **10**, 4304 (2020).
77. B. B. Jørgensen, F. Wenzhöfer, M. Egger, R. N. Glud, Sediment oxygen consumption: Role in the global marine carbon cycle. *Earth Sci. Rev.* **228**, 103987 (2022).
78. D. E. Canfield, M. T. Rosing, C. Bjerrum, Early anaerobic metabolisms. *Phil. Trans. R. Soc. Lond. B Biol. Sci.* **361**, 1819–1836 (2006).
79. J. F. Sauvage, The contribution of water radiolysis to marine sedimentary life. *Nat. Comm.* **12**, 1297 (2021).
80. R. Milo, What is the total number of protein molecules per cell volume? A call to rethink some published values. *Bioessays* **35**, 1050–1055 (2013).
81. A. Bar-Even *et al.*, The moderately efficient enzyme: Evolutionary and physicochemical trends shaping enzyme parameters. *Biochemistry* **50**, 4402–4410 (2011).
82. W. Liebermeister *et al.*, Visual account of protein investment in cellular functions. *Proc. Nat. Acad. Sci. U.S.A.* **111**, 8488–8493 (2014).
83. M. Kurr *et al.*, Methanopyrus kandleri, gen. and sp. nov. represents a novel group of hyperthermophilic methanogens, growing at 110 C. *Arch. Microbiol.* **156**, 239–247 (1991).